An Experimental and Computational Study on the Effect of Al(O*i*Pr)$_3$ on Atom-Transfer Radical Polymerization and on the Catalyst—Dormant-Chain Halogen Exchange

Rinaldo Poli,*[a] François Stoffelbach,[b] Sébastien Maria,[a] and José Mata[a]

Abstract: Compound Al(O*i*Pr)$_3$ is shown to catalyze the halide-exchange process leading from [Mo(Cp)Cl$_2$(*i*PrN=CH−CH=N*i*Pr)] and CH$_3$CH(X)COOEt (X = Br, I) to the mixed-halide complexes [Mo(Cp)ClX(*i*PrN=CH−CH=N*i*Pr)]. On the other hand, no significant acceleration is observed for the related exchange between [MoX$_3$(PMe$_3$)$_3$] (X = Cl, I) and PhCH(Br)CH$_3$, by analogy to a previous report dealing with the Ru^{II} complex [RuCl$_2$(PPh$_3$)$_3$]. A DFT computation study, carried out on the model complexes [Mo(Cp)Cl$_2$(PH$_3$)$_2$], [MoCl$_3$(PH$_3$)$_3$], and [RuCl$_2$(PH$_3$)$_3$], and on the model initiators CH$_3$CH(Cl)COOCH$_3$, CH$_3$Cl, and CH$_3$Br, reveals that the 16-electron Ru^{II} complex is able to coordinate the organic halide RX in a slightly exothermic process to yield saturated, diamagnetic [RuCl$_2$(PH$_3$)$_3$(RX)] adducts. The 15-electron [MoCl$_3$(PH$_3$)$_3$] complex is equally capable of forming an adduct, that is, the 17-electron [MoCl$_3$(PH$_3$)$_3$(CH$_3$Cl)] complex with a spin doublet configuration, although the process is endothermic, because it requires an energetically costly electron-pairing process. The interaction between the 17-electron [Mo(Cp)Cl$_2$(PH$_3$)$_2$] complex and CH$_3$Cl, on the other hand, is repulsive and does not lead to a stable 19-electron adduct. The [RuCl$_2$(PH$_3$)$_3$(CH$_3$X)] system leads to an isomeric complex [RuClX(PH$_3$)$_3$(CH$_3$Cl)] by internal nucleophilic substitution at the carbon atom. The transition state of this process for X = Cl (degenerate exchange) is located at lower energy than the transition state required for halogen-atom transfer leading to [RuCl$_3$(PH$_3$)$_3$] and the free radical CH$_3$. On the basis of these results, the uncatalyzed halide exchange is interpreted as the result of a competitive S$_N$i process, whose feasibility depends on the electronic configuration of the transition-metal complex. The catalytic action of Al(O*i*Pr)$_3$ on atom-transfer radical polymerization (and on halide exchange for the 17-electron half-sandwich Mo^{III} complex) results from a more favorable Lewis acid–base interaction with the oxidized metal complex, in which the transferred halogen atom is bound to a more electropositive element. This conclusion derives from DFT studies of the model [Al(OCH$_3$)$_3$]$_n$ (n = 1,2,3,4) compounds, and on the interaction of Al(OCH$_3$)$_3$ with CH$_3$Cl and with the [Mo(Cp)Cl$_3$(PH$_3$)$_2$] and [RuCl$_3$(PH$_3$)$_3$] complexes.

Keywords: density functional calculations · halide exchange · halogen-atom transfer · Lewis acids · polymerization

Introduction

Atom-transfer radical polymerization (ATRP) was introduced in 1995[1,2] and has since become the most actively investigated controlled radical polymerization process. With this technique, the importance of the bimolecular termination step is reduced relative to the chain propagation: the reactive radicals are in a rapid and thermodynamically favorable atom-transfer equilibrium through the action of a halogenated spin trap M−X, producing halogen-terminated dormant chains R−X (Scheme 1).

Species M is a transition-metal complex that is capable of increasing its formal oxidation state and coordination number by one unit. Since, according to Scheme 1, it is reversibly regenerated after each sequence of activation, monomer insertion(s), and deactivation processes, its effective role is that of catalyzing the polymer chain growth out of the dormant species. Thus, ATRP depends critically on

[a] Prof. R. Poli, S. Maria, Dr. J. Mata
Laboratoire de Chimie de Coordination, UPR CNRS 8241
205 Route de Narbonne, 31077 Toulouse Cedex (France)
Fax: (+33) 561-553-003
E-mail: poli@lcc-toulouse.fr

[b] F. Stoffelbach
Laboratoire de Synthèse et d'Electrosynthèse Organométalliques
Faculté des Sciences "Gabriel"
Université de Bourgogne, 6 Boulevard Gabriel
21000 Dijon (France)

 DOI: 10.1002/chem.200401143

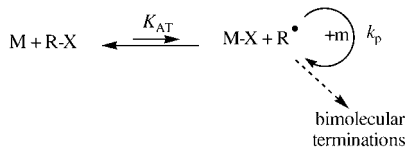

Scheme 1.

transition-metal catalysis and a number of studies have been devoted to understanding its mechanistic details.[3,4]

Of particular interest for the present study, the addition of certain Lewis acids, most notably $Al(OiPr)_3$, in conjunction with a number of catalysts has been shown to result in faster polymerization. This effect seems rather general, since it was shown for many different complexes based on a variety of different transition metals from Groups 6 to 11, including $[Mo(Cp)Cl_2(iPrN{=}CH{-}CH{=}NiPr)]$,[5] $[MoX_3(PMe_3)_3]$,[6] $[ReIO_2(PPh_3)_2]$,[7] $[Fe(Cp)X(CO)_2]$ (X = Br, I),[8] $[RuCl_2(PPh_3)_3]$,[9] $[NiBr_2(PPh_3)_2]$,[10] $[Ni(PPh_3)_4]$,[11] and [CuBr/bipy].[12] The detailed mechanism of action of this additive, however, is not completely understood. A detailed study on the effect of $Al(OiPr)_3$ for the $[RuCl_2(PPh_3)_3]$-catalyzed polymerization of methyl methacrylate demonstrated that the compound does not significantly interact with the monomer, the initiator/dormant chain, the catalyst, or the growing free radical.[9] The only noticeable effect, from a cyclic voltammetric study of the catalyst, seemed to be the stabilization of the oxidized metal complex. In the absence of the Al additive, the Ru^{II} complex shows an irreversible oxidation wave "in most cases", whereas in its presence it becomes reproducibly reversible. It is puzzling, however, that "sometimes a reduction wave appeared", even in the absence of the Al additive. A way to rationalize this irreproducibility is to envisage an irreversible interaction between the oxidation product M^+ and adventitious Lewis basic impurities, whereas this process would not occur in the presence of the Lewis acidic Al scavenger. We have recently observed similar phenomena for another system.[6] At any rate, the nature of the radical trap in the ATRP process (i.e., MX in Scheme 1) is different from the one-electron oxidation product observed in the cyclic voltammogram (M^+). Thus, the cyclic voltammetric results for complex $[RuCl_2(PPh_3)_3]$ are not directly relevant for the rationalization of the accelerating effect by the $Al(OiPr)_3$ additive.

The apparent radical polymerization rate constant takes the form of Equation (1), which contains the concentrations of the various species participating in the atom-transfer equilibrium of Scheme 1, the propagation rate constant k_p, and the atom-transfer equilibrium constant K_{AT}.

$$k_{app} = k_p K_{AT}[M][RX]/[MX] \quad (1)$$

There are only two ways in which compound $Al(OiPr)_3$ (or any other additive, for that matter) can affect this apparent rate constant: 1) by accelerating the propagation rate (increase of k_p) or 2) by shifting the atom-transfer equilibrium. A previous study has shown that conventional free-radical polymerization of methyl methacrylate (MMA) is not affected by $Al(OiPr)_3$.[9] As far as shifting the atom-transfer equilibrium, since the concentrations of M and RX cannot possibly be increased by the addition of the Al compound, the only remaining possibility is a decrease of the MX concentration, as may be accomplished by involving this species in another equilibrium.

We have therefore based our working hypothesis on the existence of a selective interaction between $Al(OiPr)_3$ and the product of the atom-transfer process, the spin trap MX. Of relevance to this phenomenon, parallel work has shown that $Al(OiPr)_3$ has no effect on the halide-exchange rate between the $[RuCl_2(PPh_3)_3]$ catalyst and a bromide initiator, $(CH_3)_2C(COOMe)CH_2C(Br)(COOMe)CH_3$.[13] This is a relevant observation because the simplest possible halide-exchange mechanism involves ATRP intermediates, see Scheme 2. Thus, the fact that $Al(OiPr)_3$ accelerates ATRP

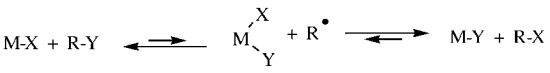

Scheme 2.

but not halide exchange may, in principle, appear puzzling. Sawamoto et al. have made the proposition that the atom-transfer process leads to an *inner sphere* radical species, $[Ru^{III}\text{-}X,R^{\cdot}]$, which is capable of undergoing fast halide exchange but leads to slow monomer insertion, whereas the presence of the aluminum compound would favor the formation of an *outer sphere* radical species, $[Ru^{III}\text{-}X/Al{+}R^{\cdot}]$, leading to faster insertion, see Scheme 3. The nature of the Ru^{III}-X/Al adduct, however, was not further speculated.[9,13]

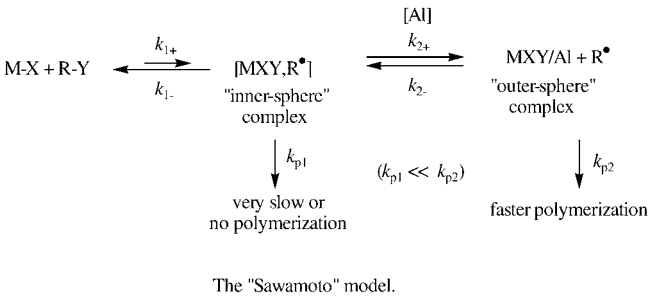

Scheme 3.

Recent work in our laboratory on compound $[Mo(Cp)Cl_2(iPrN{=}CH{-}CH{=}NiPr)]$ has shown that compound $Al(OiPr)_3$ not only accelerates the ATRP of styrene and acrylates, but also catalyzes halide exchange between the catalyst molecule and the halide initiator ethyl 2-iodopropionate (IEA). This result cannot be easily rationalized on the basis of Scheme 3. It has been reported in a preliminary communication[14] and tentatively rationalized on the basis of an independent and nonradical pathway for halide exchange, which can be operative for the 16-electron $[RuCl_2(PPh_3)_3]$ system,

but cannot take place for the 17-electron half-sandwich Mo complex. This alternative halide-exchange mechanism was proposed to consist of an internal nucleophilic substitution (S_Ni) at carbon, activated by coordination of the initiator molecule to the metal center. For the 17-electron system, coordination of the initiator to the transition-metal center is made unfavorable by the unavailability of a metal-based, low-energy, empty orbital to host the two electrons coming from a halide lone pair. Thus, the only possibility remaining for the halide-exchange pathway is the higher energy, Al(O*i*Pr)$_3$-catalyzed pathway of Scheme 2.

The purpose of the present contribution is to: 1) extend the observations of the Al(O*i*Pr)$_3$ catalytic effect (or lack thereof) on halide exchange to other ATRP catalysts used in our laboratory; 2) to provide computational support for the initiator coordination to the ATRP catalyst and for the alternative halide-exchange mechanism; 3) to analyze how compound Al(O*i*Pr)$_3$ may be capable to stabilize the spin trap, thereby shifting the atom-transfer equilibrium and accelerating ATRP.

Results

Interaction between Al(O*i*Pr)$_3$ and various compounds: The [Mo(Cp)X$_2$(*i*Pr$_2$dad)] (X = Cl, I; *i*Pr$_2$dad = 1,4-diisopropyl-1,4-diaza-1,3-butadiene, *i*PrN=CH−CH=N*i*Pr) complexes were shown to be capable of controlling the ATRP of styrene and acrylates.[5,14] Complexes [MoX$_3$(PMe$_3$)$_3$] (X = Cl, Br, I) are also capable of controlling the ATRP of styrene.[6,15] For both families of ATRP catalysts, the addition of compound Al(O*i*Pr)$_3$ to the catalytic system was found to speed up the polymerization process by a factor between 3 and 13, depending on the nature of the halides.[5,6] To probe the possible effect of the Al additive, the interactions of this compound with catalyst, monomer, and initiator were carried out.

The 17-electron complexes [Mo(Cp)X$_2$(*i*Pr$_2$dad)] (X = Cl, I) are characterized by sharp EPR signals in isotropic solutions at room temperature.[14,16] An EPR study of a solution of the dichloride complex in toluene, in the presence of an equivalent amount of the Al(O*i*Pr)$_3$ compound, at 80 °C (conditions used for the ATRP of methyl acrylate (MA)[5]) reveals no change of shape nor intensity over 1 h. The 15-electron [MoX$_3$(PMe$_3$)$_3$] complexes do not show any EPR activity in isotropic solutions at room temperature. However, in spite of their paramagnetism, they display highly shifted and broad but readily visible resonances in the ^{1}H NMR spectrum.[17] The addition of one equivalent of Al(O*i*Pr)$_3$ to a solution [MoCl$_3$(PMe$_3$)$_3$] in C$_6$D$_6$ at 65 °C for 8 h does not yield any visible change of the solution NMR spectroscopic properties.

^{1}H NMR studies have also been carried out on solutions containing Al(O*i*Pr)$_3$ and styrene (in C$_6$D$_6$ at 65 °C for 8 h, [S]/[Al] = 1/1) as well as on solutions containing compound Al(O*i*Pr)$_3$ and each of the initiators IEA and (1-bromoethyl)benzene (BEB) (in C$_6$D$_6$ at 65 °C for 8 h, [initiator]/[Al] = 1/1). In all these cases, once again, no evidence was obtained for the existence of any interaction engaging the Al(O*i*Pr)$_3$ compound. These results parallel those of analogous studies conducted on the individual components of the [RuCl$_2$(PPh$_3$)$_3$]-catalyzed MMA polymerization.[9]

Halide exchange for the 17-electron [Mo(Cp)X$_2$(*i*Pr$_2$dad)] system: During the ATRP catalyzed by the dichloride complex and by using the iodine-containing IEA initiator, the possibility exists for halide exchange between the Mo catalyst and the initiator molecule. This exchange process was investigated qualitatively by EPR spectroscopy as shown in Figure 1. Under conditions identical to those of the ATRP of MA, except that no monomer was present, the [Mo(Cp)Cl$_2$(*i*Pr$_2$dad)] displays the EPR spectrum shown in Figure 1a. No change of this spectrum (including its intensity) is evident after heating for 1 h at 80 °C, indicating the absence of halide exchange with IEA under these conditions. When the same experiment was carried out in the presence of one equivalent of Al(O*i*Pr)$_3$, on the other hand, a new resonance was evident at a greater g value relative to that of the initial catalyst, see Figure 1b. This resonance belongs to the product of halide exchange, [Mo(Cp)ICl(*i*Pr$_2$dad)], as verified by a comparison study with the products of the interaction between [Mo(Cp)Cl$_2$(*i*Pr$_2$dad)] and NaI (g = 2.010 for [Mo(Cp)ICl(*i*Pr$_2$dad)]; 2.042 for [Mo(Cp)I$_2$(*i*Pr$_2$dad)]).[14]

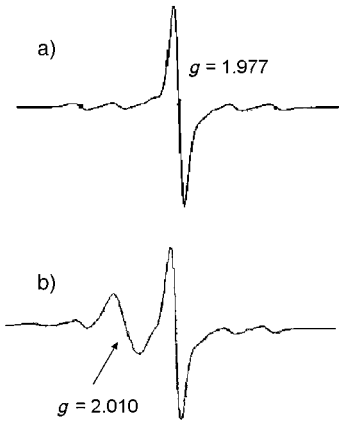

Figure 1. EPR study of complex [Mo(Cp)Cl$_2$(*i*Pr$_2$dad)] (1.4×10^{-2} M) in toluene. a) After 1 h at 80° with one equivalent of IEA (spectrum of the dichloride complex); b) same conditions as in a), except for the presence of one equivalent of Al(O*i*Pr)$_3$.

An identical experiment was carried out by using ethyl 2-bromopropionate (BrEA), with identical qualitative results, though the exchange process was faster. The results are shown in Figure 2. Unlike the experiment carried out with IEA, a slow exchange is observed even in the absence of Al additive, compare the spectrum in Figure 2a with that shown in Figure 1a. However, the process is once again greatly accelerated by Al(O*i*Pr)$_3$. The new peak observed at g = 1.991 in Figure 2b is attributed to the mixed halide complex [Mo(Cp)ClBr(*i*Pr$_2$dad)], and the broader feature observed at higher g values is certainly due to the double exchange

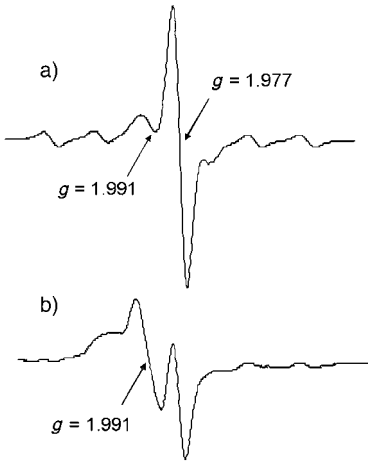

Figure 2. EPR study of complex $[Mo(Cp)Cl_2(iPr_2dad)]$ (1.6×10^{-2} M) in toluene. a) After 50 min at 80° with one equivalent of BrEA; b) same conditions as in a), except for the presence of one equivalent of $Al(OiPr)_3$.

product, $[Mo(Cp)Br_2(iPr_2dad)]$, showing that a greater extent of exchange has occurred relative to the IEA experiment, compare with Figure 1b. Although neither the mixed-halide nor the dibromide products were isolated, the positive shift of the g parameter upon replacement of Cl with the heavier halides in the order Cl < Br < I parallels exactly the shift reported for the related family of $[Mo(Cp)X_2(PMe_3)_2]$ complexes ($g=1.982$ for X = Cl, 2.006 for X = Br and 2.046 for X = I),[14] whereas the g value for the mixed $[Mo(Cp)ICl(PMe_3)_2]$ complex is 2.015.[18]

The results of these experiments demonstrate that compound $Al(OiPr)_3$ catalyzes the halide exchange between $[Mo(Cp)Cl_2(iPr_2dad)]$ and $CH_3CHXCOOEt$ (X = Br, I). As analyzed in the introduction, the most logical mechanistic hypothesis is that an atom transfer occurs, followed by recombination between the free radical and a different halide ligand from the high-oxidation-state metal complex. Since $Al(OiPr)_3$ does not seem to show any interaction with the catalyst, monomer, or initiator, it seems likely that the catalytic action is exerted via a selective thermodynamic stabilization of the spin trap. The way in which this interaction may occur will be examined in a later section.

Halide exchange for the 15-electron $[MoX_3(PMe_3)_3]$ system: Since the styrene polymerizations catalyzed by the $[MoX_3(PMe_3)_3]$ complexes were carried out with the (1-bromoethyl)benzene (BEB) initiator,[6] halide-exchange tests on this system were carried out with the same initiator. The exchange process was monitored by using both the trichloride and the triiodide complex, in the absence and in the presence of one equivalent of $Al(OiPr)_3$ per equivalent of Mo. The ^{1}H NMR resonances of the Mo complexes are not sufficiently dependent on the nature of the halides and the possibility of multiple exchange to afford all possible $[MoX_nY_{3-n}(PMe_3)_3]$ species complicates further the NMR monitoring of the transition-metal complex resonances. The exchange reactions could be conveniently monitored, in this case, by following the methyne and methyl proton resonances of the initiator by ^{1}H NMR spectrometry, since these resonances are dependent on the halide nature (for instance, the methyne resonance is at $\delta=4.85$ ppm for X = Cl, 4.75 ppm for X = Br, and 5.02 ppm for X = I), see an example in Figure 3.

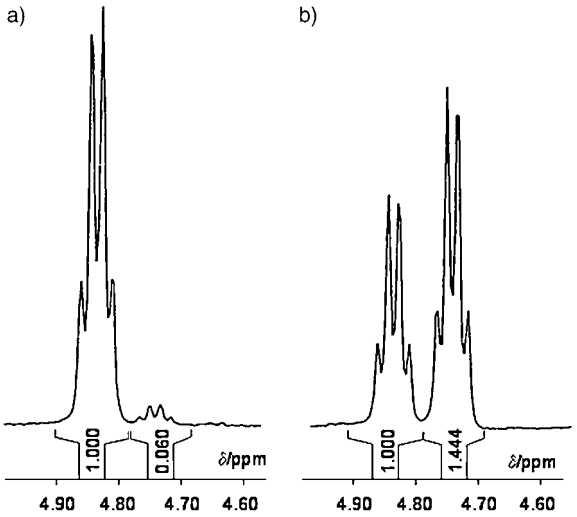

Figure 3. Examples of ^{1}H NMR spectra obtained during the halide exchange between $[MoCl_3(PMe_3)_3]$ (4×10^{-2} M) and BEB (1 equiv) at 65 °C in C_6D_6: a) after 20 min; b) after 450 min.

The results of these experiments are shown in Figure 4. Since, for technical reasons (solubility and rate), the reactions could not be carried out under pseudo-first-order conditions, and since the second-order conditions lead to complications due to the possibility of multiple exchange, no precise kinetic information could be extracted from these monitoring and the results must necessarily be considered only of qualitative value. However, it is rather clear from Figure 4 that the presence of $Al(OiPr)_3$, contrary to the 17-electron systems analyzed in the previous section, have at best only a very minor effect on the halide-exchange rate. For the $[MoCl_3(PMe_3)_3]$/BEB system, the exchange process turns out in fact as slightly *slower* in the presence of the Al additive than in its absence. For the $[MoI_3(PMe_3)_3]$/BEB

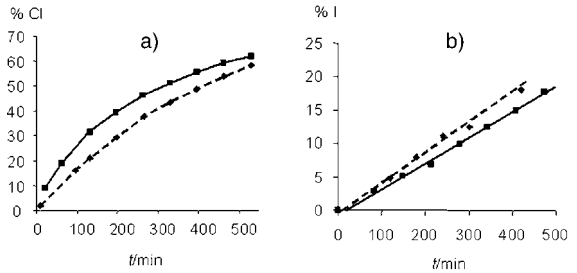

Figure 4. Results of the halide-exchange monitoring in the absence (solid line, squares) or presence (broken line, diamonds) of $Al(OiPr)_3$ at 65 °C in C_6D_6. a) $[MoCl_3(PMe_3)_3]$ (4×10^{-2} M) and BEB (1 equiv). b) $[MoI_3(PMe_3)_3]$ (1.4×10^{-2} M) and BEB (1 equiv).

system, on the other hand, the exchange is marginally faster for the experiment carried out in the presence of $Al(OiPr)_3$. The observed variations are probably caused by concentration errors, due to the need to measure rather small quantities of the reagents in each experiment.

We can therefore conclude that the halide-exchange process between the 15-electron $[MoX_3(PMe_3)_3]$ complexes and BEB is not catalyzed by $Al(OiPr)_3$ and that this process probably occurs by the same mechanism as for $[RuCl_2(PPh_3)_3]$, which is different than the mechanism operating for the 17-electron $[Mo(Cp)X_2(iPr_2dad)]$ system. The electronic configuration of the 15-electron $[MoX_3(PMe_3)_3]$ complexes is different from that of the 16-electron $[RuCl_2(PPh_3)_3]$ complex, as shown in Figure 5. The Ru^{II} complex,

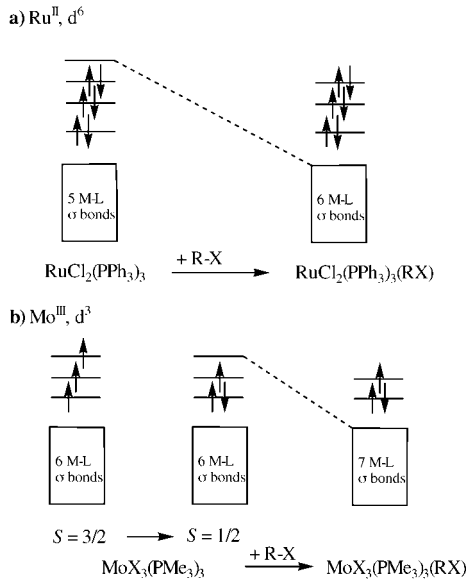

Figure 5. Schematic representation of the electronic structure evolution during the process of RX coordination to a) $[RuCl_2(PPh_3)_3]$ and b) $[MoX_3(PMe_3)_3]$.

which has a diamagnetic ground state, possesses a metal-based, low-energy, empty orbital (which is only tied up in a weak Mo–Cl π interaction), to be used to host the two electrons donated by the RX ligand, see Figure 5a. The Mo^{III} complex, on the other hand, is characterized by a spin quartet ground state (pseudo-$(t_{2g})^3$ for the approximately octahedral geometry) and no empty metal orbital is available. However, such a necessary orbital may be generated by a process of electron pairing, to yield a spin doublet configuration, see Figure 5b.

Calculations of R–X coordination, atom transfer, and halide exchange with model compounds: On the basis of the results presented above and our previously formulated hypothesis,[14] the initiator molecule should be able to coordinate to the 15-electron $[MoX_3(PMe_3)_3]$ and 16-electron $[RuCl_2(PPh_3)_3]$ complexes, but not to the 17-electron $[Mo(Cp)Cl_2(iPr_2dad)]$ complex. This proposition was investigated with the help of DFT calculations on model compounds. For the 15-electron species, we used PH_3 in place of PMe_3 and we limited our study to the trichloride complex. For the 16-electron species, we used again the model PH_3 ligand. Finally, in order to model the 17-electron system, we elected to use again a phosphine-substituted complex, $[Mo(Cp)Cl_2(PH_3)_2]$. This choice was suggested by the fact that the isoelectronic complex $[Mo(Cp)Cl_2(PMe_3)_2]$ was also shown to catalyze the polymerization of styrene by ATRP,[19] and by the fact that the product of atom transfer, the 18-electron organometallic Mo^{IV} species $[Mo(Cp)Cl_3(PMe_3)_2]$ is also a well-characterized compound,[20] whereas analogues containing dad-type ligands have not been reported so far. All optimized compounds were obtained from starting geometries adapted from crystallographically characterized analogues: $[RuCl_2(PPh_3)_3]$,[21] $[MoCl_3(PMe_2Ph)_3]$,[22] $[MoCl_4(PMe_2Ph)_3]$,[23] $[Mo(Cp)Cl_2(PMe_3)_2]$,[24] and $[Mo(Cp)Cl_3(PMe_2Ph)_2]$.[25] No structural data seem to be available for Ru^{III} complexes with the stoichiometry $[RuX_3(PR_3)_3]$ with X = any halogen. However, crystallographically characterized $[RuCl_3(L)_3]$ complexes exist, for instance with L = MeCN[26] or L_3 = terpy.[27] The optimized geometrical parameters compared quite well with the experimental data in all cases. Since this work focuses on the conceptual aspect of the $Al(OiPr)_3$ effect in ATRP, we shall not dwell on the detailed comparison of experimental and calculated structures. Our analysis will be limited to the energetic results, whereas the optimized geometric parameters will be commented only when relevant to the mechanistic discussion.

Starting with the Ru^{II} species, we have carried out the coordination study of two models of initiator molecules: compound $CH_3CHClCOOCH_3$ (as a model of the real BrEA initiator used in the Ru-catalyzed polymerization) and the simpler model CH_3Cl. The addition is found as slightly exoergic in both cases, see Figure 6. The 2.0 kcal mol^{-1} difference in favor of CH_3Cl is certainly associated to the positive inductive effect of the CH_3 group, relative to the $CH(CH_3)(COOCH_3)$ group, on the C–Cl bond, raising the energy of the Cl lone pair involved in the coordinative bond. Adding the zero-point energy and the kT correction to the data, the computed enthalpy changes for the coordination reactions at 298 K become −4.6 and −6.5 kcal mol^{-1}, respectively. Thus, both reactions are predicted to be slightly exothermic by the calculations. An alternative geometry can be envisaged for the adduct, namely that containing the halide initiator ligand in an equatorial position (*trans* to a Cl ligand). This could be conceived as deriving from the addition to a vacant site in an isomeric molecule in which a Cl ligand, rather than a PH_3 ligand, occupies the apical position. For both initiator molecules, such an isomer was computed as slightly less stable relative to the isomer shown in Figure 6, the additions to this site being exoergic by only −1.6 and −3.5 kcal mol^{-1}, respectively.

Because of computational expense, representative points at fixed C–Cl distances along the atom-transfer coordinate were calculated only for the CH_3Cl initiator, as shown in Figure 6. The transition state along the curve was located at

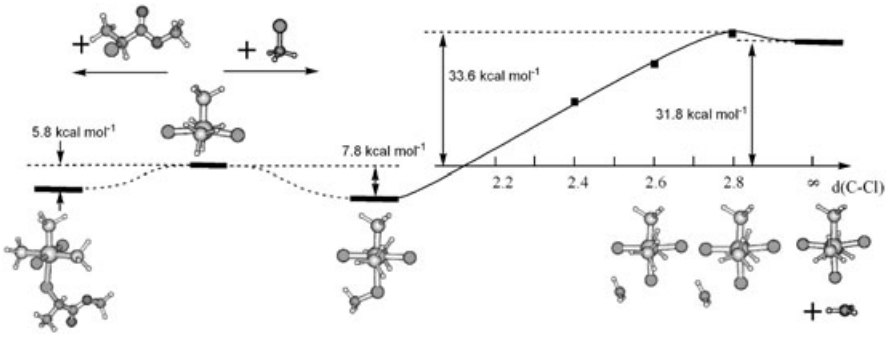

Figure 6. DFT energetic results for the coordination of $CH_3CHClCOOCH_3$ and CH_3Cl to $[RuCl_2(PH_3)_3]$, and for the Cl atom transfer from CH_3Cl.

about 33.6 kcal mol^{-1} from the sum of the free $[RuCl_2(PH_3)_3]$ and CH_3Cl molecules (41.4 kcal mol^{-1} from the adduct), while the sum of the two reaction products are located at 31.8 kcal mol^{-1} from the separated reagents (39.6 kcal mol^{-1} from the adduct). The C–Cl distance at the transition state is 2.80 Å, whereas the Ru–Cl distance is 2.45 Å, closer to the value of the same distance in the final Ru^{III} product (2.39 Å) than to that in the Ru^{II}–CH_3Cl adduct (2.68 Å). For comparison, the other two Ru–Cl distances (*trans* to each other) are 2.41 Å in the the final product and 2.46 Å in the Ru^{II} precursor. This transition state is located only 1.8 kcal mol^{-1} higher in energy than the sum of the free radicals $[RuCl_3(PH_3)_3]$ and CH_3, thus the reverse atom-transfer process (radical deactivation) is predicted to be very fast. This is a necessary condition for good control in ATRP.

Two halide-exchange processes have been investigated computationally. Once again, in order to limit the computational time factor, the transition states were calculated only for the CH_3-containing initiator molecules. The results for both processes are illustrated in Figure 7. The first process is a degenerate exchange in which the axially coordinated CH_3Cl ligand in the 18-electron adduct transfers its methyl group to one of the two equatorial Cl ligands, leading to the isomeric $[RuCl_2(PH_3)(eq\text{-}CH_3Cl)]$ adduct. The transition state for this process is located at 40.2 kcal mol^{-1} relative to the CH_3Cl adduct. This is marginally higher in energy relative to the atom-transfer products (39.6 kcal mol^{-1}), but slightly *lower* than the transition state leading to them (41.4 kcal mol^{-1}). The geometry of this transition state (TS), shown in Figure 7, is significantly different than that of the TS leading to the atom-transfer product, which is shown in Figure 6. Notably, the methyl C atom is exactly at the same distance from the two Cl atoms (2.63 Å), it retains a more pyramidalized geometry (sum the H-C-H angles = 352.1°; compare with 359.5° in the other TS), and the Ru coordination geometry is more distorted in order to bring both Cl atoms involved in the exchange closer to the methyl group (Cl-Ru-Cl angle = 82.9°, compare with 92.1° in the atom-transfer TS). The Cl-exchange TS structure was verified to contain only one imaginary frequency (380i cm^{-1}), which corresponds to the movement of the CH_3 group from the axial to the equatorial Cl atom.

The second computed exchange process consisted of a closer model of the experimentally observed Cl/Br exchange. Starting from $[RuCl_2(PH_3)_3]$, a molecule of CH_3Br was added to the vacant apical position to obtain $[RuCl_2(PH_3)_3(ax\text{-}CH_3Br)]$, a process that is exoergic by 13.9 kcal mol^{-1} (exothermic by 12.6 kcal mol^{-1} at 298 K). Thus, CH_3Br is a stronger ligand than CH_3Cl for the Ru^{II} center. From this adduct, transfer of a Me group to one of the two equivalent Cl atoms leads to $[RuClBr(PH_3)_3(eq\text{-}CH_3Cl)]$, with the stereochemistry illustrated in Figure 7, a process which is endoergic by 3.8 kcal mol^{-1}. This process occurs via a TS located 38.7 kcal mol^{-1} higher in energy, whose geometric characteristic are quite analogous to those of the TS for the degenerate Cl exchange. The single imaginary frequency has in this case the value of 366.9i cm^{-1}, while the Cl-Ru-Br angle is 89.4°. The wider value of this angle relative to the TS for the degenerate Cl exchange is related to the larger radius of the Br ligand (Br–C = 2.79 Å; Cl–C = 2.68 Å). This diminished distortion is probably the main reason for the slightly lower activation barrier in this case. We have not carried out, in this case, calculations at frozen Br–C distances along the atom-transfer coordinate. However, the final point of this curve (sum of the free $[RuCl_2Br(PH_3)_3]$ and CH_3 radicals) is 38.8 kcal mol^{-1} higher in energy relative to the

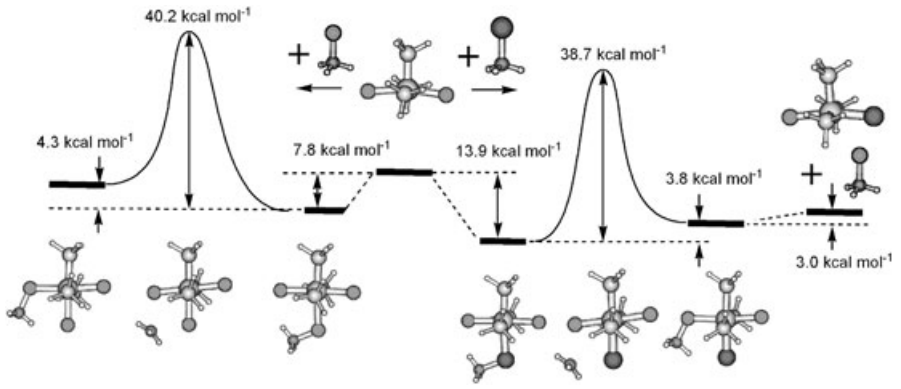

Figure 7. DFT energetic results for the halide-exchange process between $[RuCl_2(PH_3)_3]$ and CH_3Cl (degenerate exchange, left) or CH_3Br (right).

$[RuCl_2(PH_3)_3(ax\text{-}CH_3Br)]$ adduct. As for the case of the Cl atom transfer from CH_3Cl, a slight overbarrier will probably be present along the Br atom-transfer pathway. Therefore, the halide-exchange TS is located lower in energy than the atom-transfer TS. The methyl group in transit has developed a carbocationic character at the TS level according to the calculations. An NBO (NBO = natural bond order)[28] localized charge-density analysis shows that the charge of the CH_3 group increases from 0.135 in $[RuCl_2(PH_3)_3(ax\text{-}CH_3Cl)]$ to 0.304 in the TS, and then decreases back to 0.152 in $[RuCl_2(PH_3)_3(eq\text{-}CH_3Cl)]$. For the Cl/Br exchange pathway, the values are 0.076 for $[RuCl_2(PH_3)_3(eq\text{-}CH_3Br)]$, 0.280 for the TS, and 0.140 for $[RuClBr(PH_3)_3(eq\text{-}CH_3Br)]$. On the other hand, a spin unrestricted calculation on the transition-state geometries yield zero spin densities for all atoms, indicating that neither the Ru complex nor the migrating CH_3 group develop any radical character. In conclusion, this computational study validates the hypothesis that coordination of the halide initiator molecule to the Ru^{II} center in $[RuCl_2(PPh_3)_3]$ activates the halogen-carrying C atom towards an internal nucleophilic substitution, S_Ni.

Moving on to the next system, the interaction between the 17-electron model system $[Mo(Cp)Cl_2(PH_3)_2]$ and compound CH_3Cl, which was chosen again as a model of an ATRP initiator, did not lead to any stable local minima for a 19-electron adduct. This is certainly not the result of a steric problem, because compounds with an analogous coordination sphere are known for Mo^{IV}, which has a smaller ionic radius than Mo^{III}. Any attempt to place the CH_3Cl ligand either in the axial position or in an equatorial position of a putative $[Mo(Cp)Cl_2(PH_3)(CH_3Cl)]$ molecule, by using a starting geometry adapted from $[Mo(Cp)Cl_3(PH_3)_2]$, inevitably led to the expulsion of the CH_3Cl molecule far away from the coordination sphere, ultimately yielding energy and geometries corresponding to the sum of free $[Mo(Cp)Cl_2(PH_3)] + CH_3Cl$.

The energetic pathway corresponding to the Cl atom-transfer process is shown in Figure 8. In this case, stretching of the CH_3–Cl bond must start when the initiator is still quite far away from the metal center. The curve therefore acquires a rather repulsive character, while the Mo–Cl distance is still rather long. The best approach of the initiator is found from the same side as the Cp ring. An abrupt change in orientation occurs when the CH_3–Cl bond is stretched beyond 2.35 Å, corresponding to the incipient formation of the new Mo–Cl bond. The highest energy along the atom-transfer pathway (44.5 kcal mol^{-1}) corresponds to a C–Cl distance of 2.4 Å, whereas the final products are at 39.8 kcal

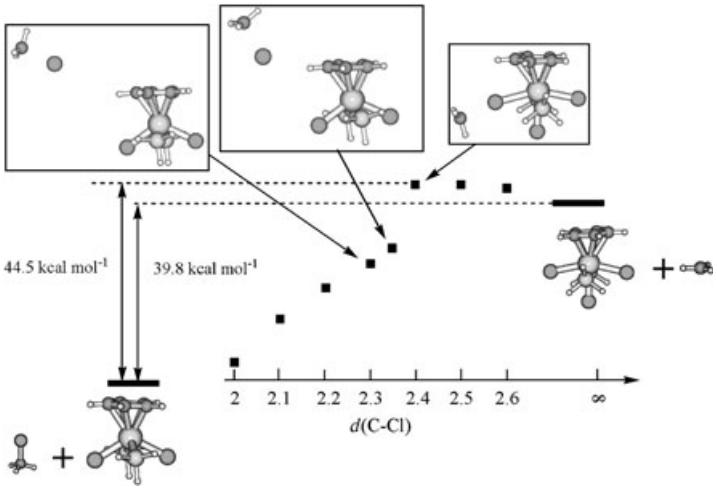

Figure 8. DFT energetic results for the Cl atom transfer from CH_3Cl to $[Mo(Cp)Cl_2(PH_3)_2]$.

mol^{-1} relative to the starting materials. Therefore, the overbarrier is worth 4.7 kcal mol^{-1} in this case. This is significantly higher than for the Ru case examined above, meaning that the $[Mo(Cp)Cl_3(PH_3)_2]$ system should lead to a slower deactivation rate than the $RuCl_3(PH_3)_3$ systems. However, these values are not highly significant, since the substituents in the real systems may have a rather large effect on these barriers.

The last system to be examined, the 15-electron $[MoCl_3(PH_3)_3]$, gives the results shown in Figure 9. The coordination of either CH_3Cl or $CH_3CHClCOOCH_3$ affords a 17-electron species with a spin-doublet ground state. In contrast to the 16-electron $[RuCl_2(PH_3)_3]$ system, the coordination reaction is endoergic. This is due to the energetically costly electron-pairing process that must accompany the ligand addition. Taking this into account, the bond formation is energetically more favorable by 3.2 kcal mol^{-1} for CH_3Cl than for $CH_3CHClCOOCH_3$, similar to the difference found for the coordination to $[RuCl_2(PH_3)_2]$. In spite of the endoergic

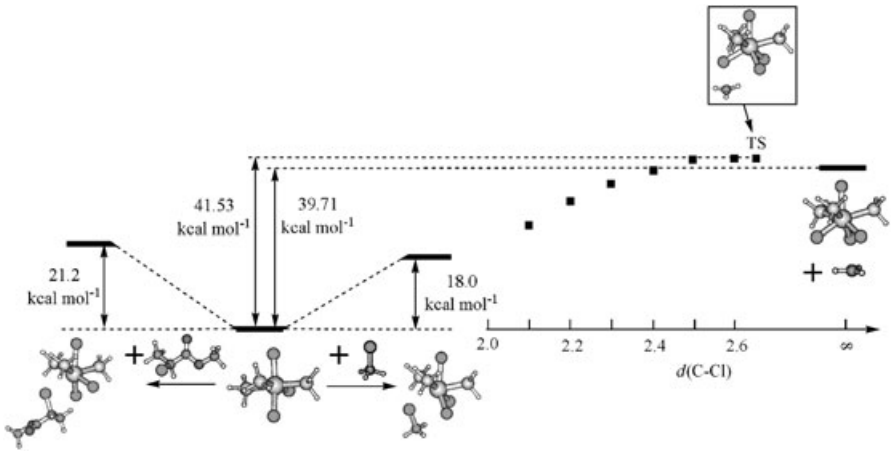

Figure 9. DFT energetic results for the Cl atom transfer from CH_3Cl to $[MoCl_3(PH_3)_3]$.

character of this coordination process, a stable local minimum is found, contrary to the 17-electron $[Mo(Cp)Cl_2(PH_3)_2]$ system. The geometry of this ligand adduct is related to that of the product of atom transfer, the 16-electron $[MoCl_4(PH_3)_3]$ complex, namely a capped octahedron in which one Cl atom acts as the capping ligand of a triangular $(PH_3)_3$ face. The initiator molecule occupies one of the positions of the opposite, uncapped triangular face together with the other two Cl atoms. The Mo–Cl distances to the coordinated initiator molecule (3.02 Å for $CH_3CHClCOOCH_3$) are significantly longer than the other Mo–Cl distances (2.40–2.56 Å), but still compatible with a genuine coordinative interaction.

As for the previously investigated systems, the atom-transfer process was investigated only for the addition of CH_3Cl. Unlike the 16-electron $[RuCl_2(PH_3)_3]$, we were unable to locate the TS of the S_Ni process. All attempts led again to the atom-transfer TS shown in Figure 9.

Calculations of $Al(OCH_3)_3$ interaction with model spin traps: The isopropoxide groups of $Al(OiPr)_3$ were modeled by methoxide. The $Al(OiPr)_3$ compound is known to exist in solution as a mixture of trinuclear and tetranuclear species.[29] However, species with lower nuclearity (dimers and even monomers) are known for analogous molecules with bulkier substituents. To learn more about the relative energetics of the various nuclearities, geometry optimizations were carried out on $[Al(OMe)_3]_n$ with $n=1$, 2, 3 and 4. The guess geometries were taken from the X-ray structures of compounds $Al[O(C_6H_2tBu_2\text{-}2,6\text{-}Me\text{-}4)]_3$,[30] $[Al(OtBu)_2(\mu\text{-}OtBu)]_2$,[31] $[Al(OCy)_2\text{-}(\mu\text{-}OCy)_2]_2Al(OCy)$,[32] and $[Al(OiPr)_2(\mu\text{-}OiPr)_2]_3Al$,[29] The energetic results are shown in Figure 10. In agreement with the known behavior, the tetranuclear and trinuclear forms were found as the most stable ones, stabilized by 42.3 and 38.6 kcal mol^{-1} (per Al atom) relative to the monomer. The greatest energetic gain is experienced on going from monomer to dimer, in which the coordination number around the Al center goes from three to four. This is because the electronic unsaturation of the Al center in the monomer (relieved only by the O lone pairs via a π-donation mechanism) is eliminated by the formation of a fourth Al–O σ bond per each Al ion in the dimer. On going from dimer to trimer, one Al ion out of three increases further its coordination number from four to five, whereas the other two Al ions maintain the same coordination environment. On going from dimer to tetramer, one Al ion out of four increases its coordination number from four to six, whereas the other three Al atoms remain four-coordinate. It is to be kept in mind that, for steric reasons, the energetic gains associated to the oligomerization of $Al(OiPr)_3$ are probably smaller relative to those calculated for $Al(OMe)_3$.

Since we are interested in evaluating the energetic effect of $Al(OiPr)_3$ on the atom-transfer equilibrium, we have calculated models of the interaction between $Al(OiPr)_3$ and the species carrying the halogen atom involved in the transfer process. As shown in Figure 10, the interaction of the model Al compound with the model initiator affords an adduct, $(MeO)_3Al\text{-}ClMe$, whose energy is lower relative to the sum of the separated species by 7.6 kcal mol^{-1}. The weakness of this interaction is signaled by the rather long Al–Cl distance (2.572 Å) and by the small pyramidal distortion of the $Al(OMe)_3$ unit (sum of the three O-Al-O angles = 355.7°). The Cl natural charge decreases only slightly from −0.083 in free CH_3Cl to −0.037 in the adduct with $Al(OMe)_3$, reflecting the weak charge transfer upon coordination to the Al center. The interaction of $Al(OMe)_3$ with the models of the spin traps $[RuCl_3(PH_3)_3]$ and $[Mo(Cp)Cl_2(PH_3)_2]$ affords adducts that are stabilized by 17.3 and 20.0 kcal mol^{-1}, respectively. The stronger interaction is experienced with the equatorial Cl ligands for both complexes, as shown in Figure 10, the interaction at the axial positions being exoergic only by 9.0 and 7.8 kcal mol^{-1}, respectively. This choice reflects the different polarization of the different M–Cl bonds, as indicated by the natural charges in the free Ru^{III} and Mo^{IV} complexes: (−0.420 vs −0.392 in the Ru^{III} complex, −0.450 vs −0.277 in the Mo^{IV} complex, for equatorial and axial positions, respectively). These charges are greater than in the CH_3Cl molecule, as may be predicted from the greater electropositive character of the metal centers. Upon coordination to the Al center, there is again a de-

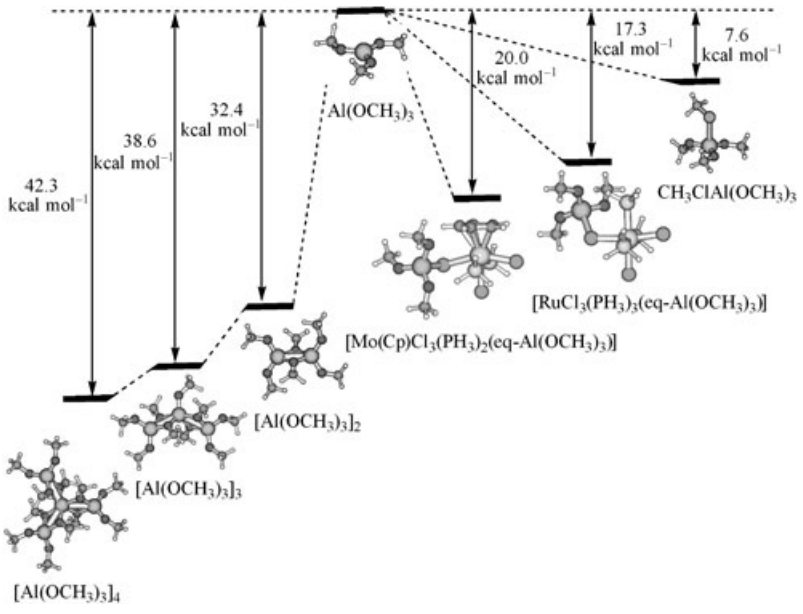

Figure 10. DFT energetic results for the interaction between $[Al(OCH_3)_3]_n$ and various compounds.

crease of natural charge at the Cl atom (from −0.420 to −0.344 for the Ru^{III} complex; from −0.450 to −0.419 for the Mo^{IV} complex). The energetically stronger Lewis acid–base interaction is also consistent with the shorter Al−Cl distance relative to the CH_3Cl−$Al(OMe)_3$ adduct (2.337 Å in the Ru^{III} complex, 2.335 Å in the Mo^{IV} complex) and with the greater degree of pyramidalization at the Al center (sum of the three O-Al-O angles = 345.46° in the Ru^{III} complex, 344.29° in the Mo^{IV} complex).

Local minima in which the Al centers establishes bonds simultaneously with two Cl ligands could not be located. Any attempt to optimize such type of structure collapsed to one of the isomeric adducts with the $Al(OMe)_3$ molecule bonded to a single Cl ligand. Thus, although the Al center is capable of increasing its coordination number up to six with bridging OMe ligands, it does not seems favorable to go beyond four-coordinate with more than one bridging Cl ligand. In summary, the calculations support the idea that the atom-transfer equilibrium shifts in favor of the higher oxidation state complex plus free radical in the presence of the Lewis acid. This phenomenon is sufficient to explain the catalytic effect of aluminum triisopropoxide on ATRP and on the halide-exchange process for the Mo^{III}(Cp) system, which follows the same atom-transfer mechanism.

The above picture should be considered only at the qualitative level. There are several phenomena that affect the quantitative value of the atom-transfer energetics. Firstly, the aluminum compound is not present in solution in the monomeric form. Even at the high temperatures used for the ATRP process, the entropic factor is not sufficiently high to generate a significant amount of monomeric species at equilibrium (by application of ZPVE, kT, and entropy corrections from the gas-phase calculation, the ΔG for the tetramer to monomer conversion affords 31.7 kcal mol^{-1} at 298 K and 29.1 kcal mol^{-1} at 398 K). Although the real isopropoxide system certainly has lower values because of the steric effect, the catalytic action is not likely to be exerted by the mononuclear species. However, the Al center is capable of expanding its coordination up to six as show by the structures of the trimer and tetramer. Therefore, the lateral, four-coordinate Al centers in the trimer and tetramer can exert their Lewis acidic action for the energetic stabilization of the atom-transfer products, though with a reduced energetic effect, along the same line shown above for the monomer. A DFT calculation for the interaction products of trimer and tetramer was not attempted given its complexity. A second complicating phenomenon is that the Al centers can also interact with the Cl atoms of the transition-metal catalyst, the Ru^{II} and Mo^{III} complex, whose natural charge is relatively high (−0.535 and −0.448, respectively). This interaction would play against the catalytic effect. However, analogous additional interactions may also occur with a second Cl ligand in the atom-transfer product. At a constant number of Al centers, therefore, the effect favors the atom-transfer products. Thirdly, the use of a simplified model for the DFT calculations may affect the value of the interaction energy. As a notable example, the close inspection of the optimized geometries of the Ru^{III} and Mo^{IV} adducts with $Al(OMe)_3$ reveals the presence of one close contact between an H atom of a PH_3 ligand and an O atom of a methoxy group (2.143 Å in the Ru^{III} complex; 2.033 Å in the Mo^{IV} complex). However, the arrangement of the $Al(OMe)_3$ moiety (M-Al-O angles, M-Al-O-C dihedral angles) and PH_3 ligands (M-P-H angles, M-P-H-O dihedral angles) do not give any clear evidence of distortions that may be associated to the formation of a hydrogen bond. Therefore, these interactions probably do not contribute significantly to the stabilization energy of the $Al(OMe)_3$ adducts, which seems to be mostly related to the strengths of the new Al−Cl bonds. The steric effect associated with the ligand simplification probably generates a greater energetic change on going from the computed model compounds to the real systems.

Discussion

The results presented above, which are subject to several approximations and assumptions, point nevertheless to a simple rationalization of the accelerating effect exerted by $Al(OiPr)_3$ on ATRP. The origin of this effect is a shift of the atom-transfer equilibrium (Scheme 1) caused by a stronger interaction between the Lewis acidic Al centers (probably the four-coordinate centers in the trimer and tetramer) with the halogen atoms in the spin trap, relative to the organic initiator. This is in turn related to the greater polarity of the metal–halogen bond in the spin trap than the carbon–halogen bond in the initiator molecule. Because of the relative weakness of these interactions, the Lewis acid–base adducts is likely to be present in solution in equilibrium with the separated species. This equilibrium is likely to be very rapid. Furthermore, because of the nature of these interactions, which involve primarily Al and Cl atoms, the spectroscopic properties probably do not change dramatically on going from the separate species to the adduct. This explains the difficulty in determining the presence of these interactions experimentally by ^{1}H NMR spectroscopy or by examining properties that are directly associated with the metal center (e.g., cyclic voltammetry, EPR for the paramagnetic complexes, …).

The appealing feature of this interpretation is that it is generally applicable to all transition-metal catalysts, since M−X bonds in the spin trap will always be more polarized than the corresponding C−X bonds in the initiator. On the basis of this interpretation, it can be easily predicted that the accelerating effect of $Al(OiPr)_3$ should be greater when the catalyst has more polarized M−X bonds. For the same halogen X, this in general occurs for higher oxidation state complexes. Indeed, the calculated strength of the $Al(OMe)_3$ interaction is greater with $[Mo(Cp)Cl_3(PH_3)_2]$, an Mo^{IV} complex, than with $[RuCl_3(PH_3)_3]$, an Ru^{III} complex.

The selective catalytic action exerted by $Al(OiPr)_3$ on the halide-exchange reaction between the ATRP catalyst and the initiator, which is function of the electronic configura-

tion of the metal, see Scheme 4, has been interpreted by the presence of two alternative halide-exchange pathways, one involving atom transfer, the second involving coordination of the initiator to an available coordination site of the transition-metal complex, followed by an internal nucleophilic substitution (S_Ni), Scheme 5. The absence of a catalytic effect by $Al(OiPr)_3$ on the S_Ni mechanism is not surprising.

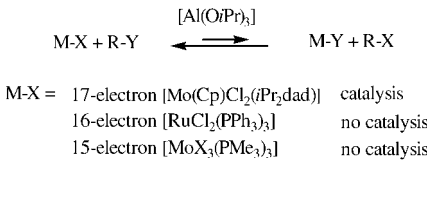

Scheme 4.

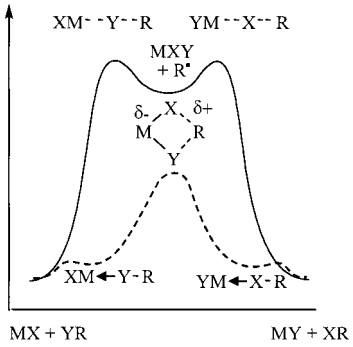

Scheme 5.

The Lewis acidic $Al(OiPr)_3$ can in principle interact only with nucleophilic centers, such as the negatively polarized halogen ligands. The S_Ni pathway involves transfer of electron density from the initiator molecule to the metal center, whose sterically crowded coordination sphere does not facilitate an electronically stabilizing interaction with the Lewis acid. The halide lone pairs need to be available to accomplish the S_Ni process, thus their involvement in a Lewis acid–base interaction with $Al(OiPr)_3$ would, if anything, exert a negative effect on the halide-exchange process. Finally, the sterically exposed migrating alkyl group has carbocationic character and is not expected to interact with the Lewis acid.

According to our interpretation, when the S_Ni pathway occurs at lower energy than the ATRP pathway, the halide-exchange process is faster than the atom-transfer process and is not catalyzed by $Al(OiPr)_3$. Conversely, when the S_Ni pathway occurs at higher energy than the ATRP pathway, both the halide-exchange and the atom-transfer processes follow the same mechanism and are both accelerated by $Al(OiPr)_3$. The proposed S_Ni mechanism is expected to take place under two conditions: 1) the initiator molecule must be capable of entering the coordination sphere of the transition metal complex, and 2) the S_Ni pathway must have a lower energy transition state than the atom-transfer pathway. The first condition cannot be satisfied by all transition-metal complexes: those with a 17-electron configuration are unlikely to coordinate weakly coordinating ligands such as organic halides and lead to 19-electron adducts, as we have verified here by DFT calculations for the model $[Mo(Cp)Cl_2(PH_3)_2]$ compound. The same situation is expected to occur for 18-electron complexes, which generally do not yield stable 20-electron adducts. However, 18-electron complexes cannot function as ATRP catalysts either, because they cannot accept the transfer of a halogen atom (a 1-electron ligand) unless another ligand dissociates first. The second condition, also, is not necessarily valid in general. It is expected to depend on the relative proximity of the two halogen atoms that are involved in the exchange (i.e., on the coordination stereochemistry) and on the nucleophilicity of the M–X bond that attacks the C atom (i.e. on the M–X bond polarity). It may be safely assumed that, if the halide-exchange process is not catalyzed by Lewis acids, as is the case here for the $[MoX_3(PMe_3)_3]$ species, then this condition is satisfied.

This scheme appears more satisfying than the outer-sphere/inner-sphere mechanism proposed by Sawamoto et al. (Scheme 3). According to this proposal, it would be necessary to assume that the "inner-sphere" {M–Y,R•} species has a sufficiently long lifetime to accomplish the uncatalyzed halide exchange, before being transformed to the "outer-sphere" counterpart under the action of $Al(OiPr)_3$, only for the 16-electron $[MoX_3Y(PMe_3)_3]$ and the 17-electron $[RuCl_2Y(PPh_3)_3]$, but not for the 18-electron $[Mo(Cp)Cl_2Y(iPr_2dad)]$. A notable difference between those species is that the 18-electron $Mo^{IV}(Cp)$ complex is diamagnetic, whereas the others have radical character ($S=1/2$ for the 17-electron Ru^{III} complex and $S=1$ for the 16-electron Mo^{IV} tetrahalide complex). Thus, one would need to assume that the organic radical escapes the transition-metal rapidly when this has no spin density and slowly when it has one or more unpaired electrons. In addition, one would have to assume that halide exchange, like monomer insertion, is faster for the "outer-sphere" complex, but only when using the 17-electron ATRP catalyst. Although we have no concrete experimental data to exclude this scenario, we cannot find any simple argument to support it. The energetic comparison of the computed transition states for atom transfer and for S_Ni halide exchange for the $[RuCl_2(PH_3)_3]$ model system persuades us that the uncatalyzed halide exchange occurs through the S_Ni pathway.

It is evident that, according to the S_Ni mechanism, the halide exchange should be accompanied by 100% retention of the absolute configuration, whereas exchange via a radical species should lead to partial loss of the enantiomeric excess, depending on the radical lifetime in the "inner-sphere" complex. Unfortunately, we could not test the stereochemistry of this halide exchange by using optically active molecules such as $CH_3CH(X)Ph$ or CH_3CH-

(X)COOEt, because of the need to carry out these processes under conditions (i.e., 65 °C) in which racemization would easily occur, at least for the more fragile bromide systems, according to the literature.[33,34] It is interesting to note that, in a previous investigation on a Cu^I system, Matyjaszewski et al. found that the rates of halide exchange, activation, and racemization were exactly the same.[35] This observation is perfectly in line with our proposed model, since the electronically saturated Cu^I complex would not allow easy access to the initiator molecule (a weak 2-electron neutral ligand) to open access to the S_Ni pathway. Thus, halide exchange can only occur through the atom-transfer pathway (Scheme 2).

Conclusion

Our calculations on model compounds suggest that the accelerating effect exerted by the $Al(OiPr)_3$ additive on ATRP is related to the establishment of a stronger Lewis acid–base interaction with the halogen atom after this is transferred from the organic initiator to the more electropositive transition-metal catalyst. As a result, the atom-transfer equilibrium is slightly shifted toward the formation of the active radical and the spin trap. This phenomenon is also responsible for the acceleration of the halide-exchange process between the initiator and the catalyst, when the latter is a 17-electron half-sandwich Mo^{III} compound. This acceleration phenomenon has been experimentally verified for the halide exchange between $[Mo(Cp)Cl_2(i\text{PrN=CH–CH=N}i\text{Pr})]$ and the $CH_3CH(X)COOEt$ (X = Br, I) initiators. On the other hand, the absence of an acceleration by $Al(OiPr)_3$, which was reported previously[13] for the halide exchange between the 16-electron $[RuCl_2(PPh_3)_3]$ and $(CH_3)_2C(COOMe)CH_2C(Br)(COOMe)CH_3$, is also found for the halide exchange between the 15-electron $[MoX_3(PMe_3)_3]$ (X = Cl, I) complexes and $PhCH(Br)CH_3$. A rationalization of this dichotomy has been presented on the basis of a nonradical, competitive halide-exchange mechanism, which is favored over the atom-transfer mechanism depending on the electronic structure of the transition-metal complex. The new mechanism consists of an internal nucleophilic substitution (S_Ni) that requires activation of the initiator C–X bond by coordination to the metal center. The feasibility of this coordination process for the $[RuCl_2(PPh_3)_3]$ and $[MoCl_3(PMe_3)_3]$ complexes (as well as its unfeasibility for the 17-electron half-sandwich Mo^{III} complex) was verified by DFT calculations on model systems. Furthermore, the reaction profile of the S_Ni process has been identified, including the geometry and energy of the transition state. This mechanistic dichotomy for the halide-exchange process is at variance with the previous proposition[13] of an inner-sphere/outer-sphere equilibrium, and appears to be broadly applicable to the interpretation and prediction of the $Al(OiPr)_3$ effect (as well as to the effect of related Lewis acidic additives) on atom-transfer and halide-exchange reactions involving transition-metal halides and organic halides.

Experimental Section

General: All operations were carried out under an atmosphere of pre-purified argon. Solvents were dried by conventional methods, deoxygenated, and distilled under dinitrogen. NMR spectra were recorded in $CDCl_3$ on a Bruker 300 Avance instrument. The spectra were calibrated with the residual solvent peaks and all resonances are reported with positive shifts downfield from $SiMe_4$. EPR measurements were carried out at the X-band microwave frequency on a Bruker ESP300 spectrometer. The spectrometer frequency was calibrated with diphenylpicrylhydrazyl (DPPH, $g = 2.0037$). Compounds $[Mo(Cp)Cl_2(i\text{Pr}_2\text{dad})]$,[16] $[MoCl_3(PMe_3)_3]$,[36] and $[MoI_3(PMe_3)_3]$[37] were prepared following published procedures. Compounds $CH_3CH(Br)COOEt$ (BrEA) and $CH_3CH(Br)Ph$ (BEB) were purchased from Aldrich and used as received. Ethyl 2-Iodopropionate (IEA) was obtained according to a previously described synthetic procedure.[38]

Reaction between $[Mo(Cp)Cl_2(i\text{Pr}_2\text{dad})]$ and $CH_3CHICOOEt$: A solution containing $[Mo(Cp)Cl_2(i\text{Pr}_2\text{dad})]$ (8.1 mg, 2.1×10^{-2} mmol) and $CH_3CHICOOEt$ (3.0 μL, 5.0 mg, 2.2×10^{-2} mmol) in toluene (1.5 mL) was split into two equal portions. To one of them was added $Al(OiPr)_3$ (2.4 mg, 1.2×10^{-2} mmol). The two solutions were transferred into 4 mm Pyrex tubes, which were flame sealed and then placed together in a heated oil bath (80 °C). The progress of the reaction was monitored by EPR spectroscopy (see Results section).

Reaction between $[Mo(Cp)Cl_2(i\text{Pr}_2\text{dad})]$ and $CH_3CH(Br)COOEt$: Following a procedure analogous to that described above, a solution containing $[Mo(Cp)Cl_2(i\text{Pr}_2\text{dad})]$ (90 mg, 0.24 mmol) and $CH_3CH(Br)COOEt$ (31.2 μL, 43.4 mg, 0.24 mmol) in toluene (15 mL) was split into two equal portions. To one of them was added $Al(OiPr)_3$ (24.7 mg, 0.12 mmol). Portions of the two solutions were transferred into 4 mm Pyrex tubes, which were flame sealed and then placed together in a heated oil bath (80 °C). The progress of the reaction was monitored by EPR spectroscopy (see Results section).

Reaction between $[MoCl_3(PMe_3)_3]$ and $CH_3CH(Br)Ph$ with $Al(OiPr)_3$: $[MoCl_3(PMe_3)_3]$ (10.7 mg, 2.49×10^{-2} mmol), BEB (3.4 μL, 4.61 mg, 2.49×10^{-2} mmol), and $Al(OiPr)_3$ (5.0 mg, 2.45×10^{-2} mmol) were dissolved in C_6D_6 (0.6 mL). The resulting solution was transferred into an NMR tube and introduced into the NMR probe maintained at 65 °C. The progress of the reaction was followed by monitoring the decrease of the *i*Pr methyne resonance for BEB ($PhCHBrCH_3$, $\delta = 4.85$ ppm) against the increase of the methyl resonance for the chloride analogue ($PhCHClCH_3$ $\delta = 1.58$ ppm). This was necessary because the methyne resonance for $PhCHClCH_3$ overlapped with one of the *i*Pr methyne resonances of $Al(OiPr)_3$.

Reaction between $[MoCl_3(PMe_3)_3]$ and $CH_3CH(Br)Ph$ without $Al(OiPr)_3$: $[MoCl_3(PMe_3)_3]$ (12.7 mg, 2.95×10^{-2} mmol) and BEB (4 μL, 5.42 mg, 2.93×10^{-2} mmol) were dissolved in C_6D_6 (0.6 mL). The resulting solution was transferred into an NMR tube and introduced into the NMR probe maintained at 65 °C. The progress of the reaction was followed by monitoring the *i*Pr methyne resonance ($PhCHXCH_3$: $\delta = 4.85$ and 4.75 ppm for X = Br and Cl, respectively).

Reaction between $[MoI_3(PMe_3)_3]$ and $CH_3CH(Br)Ph$ with $Al(OiPr)_3$: $[MoI_3(PMe_3)_3]$ (6.1 mg, 8.6×10^{-3} mmol), BEB (1.2 μL, 1.63 mg, 8.8×10^{-3} mmol), and $Al(OiPr)_3$ (2.0 mg, 9.8×10^{-3} mmol) were dissolved in C_6D_6 (0.6 mL). The resulting solution was transferred into an NMR tube and introduced into the NMR probe maintained at 65 °C. The progress of the reaction was followed by monitoring the *i*Pr methyne resonance ($PhCHXCH_3$: $\delta = 4.85$ and 5.02 ppm for X = Br and I, respectively).

Reaction between $[MoI_3(PMe_3)_3]$ and $CH_3CH(Br)Ph$ without $Al(OiPr)_3$: $[MoI_3(PMe_3)_3]$ (11.2 mg, 1.59×10^{-2} mmol) and BEB (2.2 μL, 2.98 mg, 1.61×10^{-2} mmol) were dissolved in C_6D_6 (0.6 mL). The resulting solution was transferred into an NMR tube and introduced into the NMR probe maintained at 65 °C. The progress of the reaction was monitored by ^1H NMR spectroscopy as described above.

DFT calculations: All DFT calculations were carried out with the Gaussian 03 program suite[39] by using the B3LYP functional.[40] The 6–31G* basis set was used for all C, H, O, N, Cl, and Br atoms. The Mo atom was described by the LANL2DZ basis set, to which an *f* polarization function

($\alpha = 0.8$) was added. All molecules were optimized with the spin-unrestricted formalism. The mean value of the S^2 operator was always very close to the theoretical value of 0.75 for spin doublets, 2 for spin triplets, and 3.75 for spin quartets for all optimized geometries corresponding to energy minima. A major spin contamination was only found for the TS relating the spin doublet $[MoCl_3(PMe_3)_3(ClMe)]$ to the sum of spin triplet $[MoCl_4(PMe_3)_3]$ and spin doublet CH_3 ($\langle S^2 \rangle = 1.48$), a consequence of the near degeneracy of the parallel ($S = 3/2$) and antiparallel ($S = 1/2$) arrangements. The S^2 mean value rapidly tends to 0.75 as the C–Cl distance decreases to that of the $[MoCl_3(PMe_3)_3(ClMe)]$ minimum. All geometry optimizations were performed without symmetry constraints (C_1 symmetry). The nature of the resulting stationary points as energy minima was verified by a frequency analysis in each case. All energies were corrected for zero-point vibrational energy and for thermal energy to obtain the reaction enthalpies at 298 K.

Acknowledgements

We are grateful to the CNRS for financial help. F.S. and S.M. are grateful to CNRS and to the Conseil Régional de Bourgogne for BDI fellowships, and J.M. thanks the Spanish Ministerio de Educacion y Ciencia for a post-doctoral fellowship.

[1] J.-S. Wang, K. Matyjaszewski, *J. Am. Chem. Soc.* **1995**, *117*, 5614–5615.
[2] M. Kato, M. Kamigaito, M. Sawamoto, T. Higashimura, *Macromolecules* **1995**, *28*, 1721–1723.
[3] K. Matyjaszewski, J. H. Xia, *Chem. Rev.* **2001**, *101*, 2921–2990.
[4] M. Kamigaito, T. Ando, M. Sawamoto, *Chem. Rev.* **2001**, *101*, 3689–3745.
[5] F. Stoffelbach, D. M. Haddleton, R. Poli, *Eur. Polym. J.* **2003**, *39*, 2099–2105.
[6] S. Maria, F. Stoffelbach, J. Mata, J.-C. Daran, P. Richard, R. Poli, *J. Am. Chem. Soc.*, in press.
[7] Y. Kotani, M. Kamigaito, M. Sawamoto, *Macromolecules* **1999**, *32*, 2420–2424.
[8] Y. Kotani, M. Kamigaito, M. Sawamoto, *Macromolecules* **1999**, *32*, 6877–6880.
[9] T. Ando, M. Kamigaito, M. Sawamoto, *Macromolecules* **2000**, *33*, 6732–6737.
[10] H. Uegaki, Y. Kotani, M. Kamigaito, M. Sawamoto, *Macromolecules* **1997**, *30*, 2249–2253.
[11] H. Uegaki, M. Kamigaito, M. Sawamoto, *J. Polym. Sci. Part A* **1999**, *37*, 3003–3009.
[12] J. Guo, Z. Han, P. Wu, *J. Mol. Catal. A* **2000**, *159*, 77–83.
[13] T. Ando, M. Kamigaito, M. Sawamoto, *Macromolecules* **2000**, *33*, 2819–2824.
[14] F. Stoffelbach, R. Poli, *Chem. Commun.* **2004**, 2666–2667.
[15] F. Stoffelbach, J. Claverie, R. Poli, *C. R. Acad. Chim.* **2002**, *5*, 37–42.
[16] F. Stoffelbach, R. Poli, P. Richard, *J. Organomet. Chem.* **2002**, *663*, 269–276.
[17] R. Poli, H. D. Mui, *Inorg. Chem.* **1991**, *30*, 65–77.
[18] R. G. Linck, B. E. Owens, R. Poli, A. L. Rheingold, *Gazz. Chim. Ital.* **1991**, *121*, 163–168.
[19] E. Le Grognec, J. Claverie, R. Poli, *J. Am. Chem. Soc.* **2001**, *123*, 9513–9524.
[20] F. Abugideiri, J. C. Fettinger, D. W. Keogh, R. Poli, *Organometallics* **1996**, *15*, 4407–4416.
[21] S. J. La Placa, J. A. Ibers, *Inorg. Chem.* **1965**, *4*, 778–783.
[22] K. Yoon, G. Parkin, A. L. Rheingold, *J. Am. Chem. Soc.* **1991**, *113*, 1437–1438.
[23] L. Manojlovic-Muir, *J. Chem. Soc. Dalton Trans.* **1976**, 192–195.
[24] S. T. Krueger, R. Poli, A. L. Rheingold, D. L. Staley, *Inorg. Chem.* **1989**, *28*, 4599–4607.
[25] F. Abugideiri, J. C. Gordon, R. Poli, B. E. Owens-Waltermire, A. L. Rheingold, *Organometallics* **1993**, *12*, 1575–1582.
[26] L. Appelbaum, C. Heinrichs, J. Demtschuk, M. Michman, M. Oron, H. J. Schafer, H. Schumann, *J. Organomet. Chem.* **1999**, *592*, 240–250.
[27] F. Laurent, E. Plantalech, B. Donnadieu, A. Jimenez, F. Hernandez, M. Martinez-Ripoll, M. Biner, A. Llobet, *Polyhedron* **1999**, *18*, 3321–3331.
[28] A. E. Reed, L. A. Curtiss, F. Weinhold, *Chem. Rev.* **1988**, *88*, 899–926.
[29] K. Folting, W. E. Streib, K. G. Caulton, O. Poncelet, L. G. Hubert-Pfalzgraf, *Polyhedron* **1991**, *10*, 1639–1646.
[30] M. D. Healy, M. R. Mason, P. W. Gravelle, S. G. Bott, A. R. Barron, *J. Chem. Soc. Dalton Trans.* **1993**, 441–454.
[31] R. H. Cayton, M. H. Chisholm, E. R. Davidson, V. F. Distasi, P. Du, J. C. Huffman, *Inorg. Chem.* **1991**, *30*, 1020–1024.
[32] J. Pauls, B. Neumuller, *Z. Anorg. Allg. Chem.* **2000**, *626*, 270–279.
[33] R. O. Hutchins, D. Masilamani, C. A. Maryanoff, *J. Org. Chem.* **1976**, *41*, 1071–1072.
[34] A. R. Stein, *J. Org. Chem.* **1976**, *41*, 519–523.
[35] K. Matyjaszewski, H. Paik, D. A. Shipp, Y. Isobe, Y. Okamoto, *Macromolecules* **2001**, *34*, 3127–3129.
[36] J. L. Atwood, W. E. Hunter, E. Carmona-Guzman, G. Wilkinson, *J. Chem. Soc. Dalton Trans.* **1980**, 467–470.
[37] F. A. Cotton, R. Poli, *Inorg. Chem.* **1987**, *26*, 1514–1518.
[38] D. P. Curran, E. Bosch, J. Kaplan, M. Newcomb, *J. Org. Chem.* **1989**, *54*, 1826–1831.
[39] Gaussian 03, Revision B.04, M. J. Frisch, G. W. Trucks, H. B. Schlegel, G. E. Scuseria, M. A. Robb, J. R. Cheeseman, J. A. Montgomery, Jr., T. Vreven, K. N. Kudin, J. C. Burant, J. M. Millam, S. S. Iyengar, J. Tomasi, V. Barone, B. Mennucci, M. Cossi, G. Scalmani, N. Rega, G. A. Petersson, H. Nakatsuji, M. Hada, M. Ehara, K. Toyota, R. Fukuda, J. Hasegawa, M. Ishida, T. Nakajima, Y. Honda, O. Kitao, H. Nakai, M. Klene, X. Li, J. E. Knox, H. P. Hratchian, J. B. Cross, V. Bakken, C. Adamo, J. Jaramillo, R. Gomperts, R. E. Stratmann, O. Yazyev, A. J. Austin, R. Cammi, C. Pomelli, J. W. Ochterski, P. Y. Ayala, K. Morokuma, G. A. Voth, P. Salvador, J. J. Dannenberg, V. G. Zakrzewski, S. Dapprich, A. D. Daniels, M. C. Strain, O. Farkas, D. K. Malick, A. D. Rabuck, K. Raghavachari, J. B. Foresman, J. V. Ortiz, Q. Cui, A. G. Baboul, S. Clifford, J. Cioslowski, B. B. Stefanov, G. Liu, A. Liashenko, P. Piskorz, I. Komaromi, R. L. Martin, D. J. Fox, T. Keith, M. A. Al-Laham, C. Y. Peng, A. Nanayakkara, M. Challacombe, P. M. W. Gill, B. Johnson, W. Chen, M. W. Wong, C. Gonzalez, J. A. Pople, Gaussian, Wallingford CT, **2004**..
[40] A. D. Becke, *J. Chem. Phys.* **1993**, *98*, 5648–5652.

Received: November 12, 2004
Published online: February 25, 2005